INTERNATIONAL JOURNAL FOR NUMERICAL METHODS IN FLUIDS
Int. J. Numer. Meth. Fluids 2005; **49**:171–182
Published online 16 May 2005 in Wiley InterScience (www.interscience.wiley.com). DOI: 10.1002/fld.991

Buffeting in transonic flow prediction using time-dependent turbulence model

A. Kourta[1,*,†], G. Petit[1,2], J. C. Courty[2] and J. P. Rosenblum[2]

[1]*IMFT, Av. du Prof. Camille Soula, F-31400 Toulouse, France*
[2]*Dassault-Aviation, 78, quai Marcel Dassault, 92124 Saint-Cloud, France*

SUMMARY

In transonic flow conditions, the shock wave/turbulent boundary layer interaction and flow separations on wing upper surface induce flow instabilities, 'buffet', and then the buffeting (structure vibrations). This phenomenon can greatly influence the aerodynamic performance. These flow excitations are self-sustained and lead to a surface effort due to pressure fluctuations. They can produce enough energy to excite the structure. The objective of the present work is to predict this unsteady phenomenon correctly by using unsteady Navier–Stokes-averaged equations with a time-dependent turbulence model based on the suitable (k–ε) turbulent eddy viscosity model. The model used is based on the turbulent viscosity concept where the turbulent viscosity coefficient $C\mu$ is related to local deformation and rotation rates. To validate this model, flow over a flat plate at Mach number of 0.6 is first computed, then the flow around a NACA0012 airfoil. The comparison with the analytical and experimental results shows a good agreement. The ONERA OAT15A transonic airfoil was chosen to describe buffeting phenomena. Numerical simulations are done by using a Navier–Stokes SUPG (streamline upwind Petrov–Galerkin) finite-element solver. Computational results show the ability of the present model to predict physical phenomena of the flow oscillations. The unsteady shock wave/boundary layer interaction is described.

KEY WORDS: transonic flow; buffeting; turbulence model; numerical simulation; airfoil

1. INTRODUCTION

The buffeting is the structural response to an aerodynamic excitation created by a viscous flow phenomenon existing on different parts of a body. The instabilities of the flow inducing the buffeting are natural and self-sustained. These phenomena can be observed on aircraft, turbomachine stages, rockets, etc. Even if it is not dangerous and not destructive, the buffeting

*Correspondence to: A. Kourta, IMFT, Av. du Prof. Camille Soula, F-31400 Toulouse, France.
†E-mail: kourta@imft.fr

Contract/grant sponsor: CNRS; contract/grant number: GDR2502

Received 25 January 2005
Revised 25 March 2005
Accepted 1 April 2005

can increase the structure fatigue, disturb the aircraft manoeuverability and decrease the passenger's comfort. It can have an important influence on the aerodynamic behaviour of the aircraft.

The aim of this paper is to accurately predict the buffeting and to analyse these characteristics. The buffet can appear in many flight flow conditions. It is accentuated in transonic flow by the motion of the shock wave location caused by the flow separations, when they spread from the shock to the trailing edge. In this paper only the buffet in transonic flow, shock wave/turbulent boundary layer interaction and flow separations, are described. The performed transonic flow tests have permitted a better description of the buffet [1–6]. The transonic flows are often crossed by shock waves induced by a sudden recompression of the flow. These waves interfere with the boundary layer. These interactions lead to flow separation. When the shock wave is strong enough, the separated region spreads to the trailing edge and thickens. Large-scale instabilities are then developed. The size of separated flow layer fluctuates with the shock wave location [1, 2]. The frequencies and amplitudes of these fluctuations depend on the airfoil parameters and the flow conditions. These instabilities are named 'buffet' and can produce buffeting. In these conditions, the pressure levels, and therefore the lift, strongly vary. Periodic shock motions on airfoils in transonic flows have been observed experimentally by various authors. Schlieren photographs of flowfields clearly indicate the presence of upstream moving waves originating at the trailing edge and near-wake region. They are associated with wake fluctuations due to unsteady shock motions. Several explanations of the mechanisms of shock wave oscillations have been advanced by various authors depending on experimental results obtained with different airfoils and flow conditions. A possible mechanism of the self-sustained oscillation caused by unsteady transonic shock wave/boundary layer interaction with separated flow at the shock wave is, because of the movement of the shock, pressure waves are formed which propagate downstream in the separated region. On reaching the trailing edge, the disturbances generate upstream moving waves. These waves will interact with the shock and impact energy to maintain its oscillation. The loop is then completed.

There exist, also, numerical studies for flows around airfoil in the transonic regime. Although these studies report the existence of this kind of unsteady phenomena, they investigated rather numerical aspects of these transonic flows. These transonic flows are often turbulent, so appropriate numerical simulation and suitable equations have to be used. In the aerodynamic configurations the only viable way to perform is to use averaged Navier–Stokes equations with turbulence model. However, up to now, the turbulent models used are not able to accurately predict these kind of instabilities. This work is motivated by the fact that classical Reynolds-averaged Navier–Stokes (RANS) models are not able to compute this flow correctly. The aim of this study is to use a developed suitable turbulent model to predict these oscillations and to analyse the shock wave–boundary layer interactions in transonic flows. The ONERA OAT15A airfoil was chosen. The numerical results were compared to an experiment carried out in the ONERA wind tunnel. In this experiment, the boundary layer transition was fixed at $x/c = 7\%$ on both sides of the airfoil. Experimental results show that the buffeting starts at an angle of attack of 3.25°. To show the capability of the model to predict buffeting, computations are done for an angle of attack of 4°. Computational results show the ability of the present model to predict physical phenomena of the flow oscillations. The used model presents good agreement with experimental results.

2. METHODOLOGY

2.1. Numerical method

The physical model is an unsteady RANS equation for a 2D flow and a k–ε model is modified to be used in separated and unsteady case. The coordinate system used is the Cartesian one (x, y). (For more details see Reference [7].)

The flow solver uses a finite-element method SUPG (streamline upwind Petrov–Galerkin), which is second order in space. The time integration is implicit and second order accurate [8].

The time integration uses an implicit backward differentiation formulae (BDF) scheme coupled with a dual time stepping (DTS) to accelerate a convergence. For each unsteady iteration, to accelerate the convergence, n internal iterations are done by using GMRES (general minimum residual). For these internal iterations the CFL number can be high without disturbing the computational stability. For each iteration the computation is done as

$$\underbrace{\frac{V^{n+1,\upsilon+1} - V^{n+1,\upsilon}}{\Delta\tau}}_{\text{DTS}} + \underbrace{\frac{\frac{3}{2}V_{n+1} - 2V_n + \frac{1}{2}V_{n-1}}{\Delta t}}_{\text{BDF}} = -\operatorname{Re} s(U_{n+1,\upsilon})$$

where t is a physical time and τ is the internal numerical time for a dual time stepping.

Tests are done to evaluate the accuracy of the numerical scheme by using different resolutions in time and space [9]. So, for each computation the adapted mesh and time step are selected.

2.2. Turbulent model

In transonic flow, the shock wave/turbulent boundary layer interaction leads to the flow oscillations. In this case the flow is unsteady. Direct numerical simulation (DNS) or at least large eddy simulation (LES) are proper approaches to take account of small scales within a 3D framework. However, they require an enormous amount of resources for even simple geometry. A hybrid RANS/LES approach based on blending the best features of RANS and LES can be also used. Ideally, one could adequately simulate this class of flows with adapted unsteady RANS (URANS) technique [10]. However, these turbulence models are well known to be dissipative and without caution unsteadiness can be damped. Here, the k–ε model used is adapted to this purpose.

The starting point of the present approach is the decomposition of any instantaneous physical variable into a coherent, organized part and an incoherent, random part. Equations for the coherent part are obtained by performing an ensemble average of the instantaneous flow equations. The effects of the random part are introduced by using a suitable unsteady turbulence model.

The closure law of turbulent stresses that was used is similar to the one obtained by Zhu and Shih [10], or Shih *et al.* [11], and it was used by these authors to compute steady flows. Assuming that the unknown correlations, resulting from the use of ensemble averaging, depend on the averaged velocity gradients, turbulent length, and velocity scales, a closure relation is derived by using the invariance theory. Using the realizability conditions [12], the coefficients are found to be functions of the time-scale ratio of the turbulence to the averaged strain rate and the one of the time scale of the turbulence to the averaged rotation rate. Using the

turbulent kinetic energy k and dissipation ε to characterize the turbulent length and velocity scales, the averaged turbulent correlations can be derived.

A semi-deterministic model is based on the turbulent viscosity concept (for more details see References [7, 13]). Turbulent shear stress tensor is obtained by following Boussinesq relation:

$$\tau_{ij} = -\rho\overline{u_i u_j} = 2\mu_t(S_{ij} - \tfrac{1}{3}S_{kk}\delta_{ij}) - \tfrac{2}{3}\rho k\delta_{ij}$$

The turbulent viscosity is given by:

$$\mu_t = C_\mu \rho \frac{k^2}{\varepsilon}$$

C_μ, the turbulent viscosity coefficient is related to deformation rate η and rotation rate ξ:

$$C_\mu(\eta,\zeta) = \frac{2}{3}\frac{1}{A_1 + \eta + \gamma_1\xi} \quad \text{with } \eta = \frac{k}{\varepsilon}S, \;\; \xi = \frac{k}{\varepsilon}\Omega$$

where S is the deformation and Ω is the rotation. A_1 is equal to 1.25 and γ_1 to 0.9.

To close the equations, the averaged turbulent kinetic energy and its averaged dissipation are determined from the solution of their transport equations.

For the near-wall region, the low turbulent Reynolds numbers treatment is used. The damping function is deduced from the mixing lengths l_μ and l_ε. The low Reynolds number model computes the turbulent kinetic energy k and estimates ε from the turbulent viscosity calculation:

$$l_\mu = Cl\, y\,(1 - \exp^{-Ry/A\mu})$$

$$l_\varepsilon = Cl\, y(1 - \mathrm{e}^{-Ry/A\varepsilon})$$

With: $A\mu = 72.8$, $A\varepsilon = 2\,Cl$, $\kappa = 0.41$, $Cl = \kappa C\mu^{-3/4}$ and $Ry = \rho(k^{1/2}y/\mu)$ the turbulent Reynolds number.

Hence: $\varepsilon = k^{3/2}/l_\varepsilon$ and the dumping function $f\mu = l_\mu/l_\varepsilon$ that can be used to compute the turbulent viscosity:

$$\mu_t = f\mu\, C\mu(\eta,\xi)\rho\frac{k^2}{\varepsilon}$$

2.3. *Computational conditions*

Flow conditions are the experimental ones in the S3 ONERA wind tunnel where investigations on the OAT15A airfoil were carried out [5]. OAT15A is a supercritical airfoil with a thickness to chord ratio of 12.3%, a chord length equal to 230 mm and a thick trailing edge of 0.5% of the chord length. Flow conditions were the following: $M_\infty = 0.73$, $P_i = 10^5$ bar, $T_i = 300$ K and $\mathrm{Re}_c = 2.8 \times 10^6$. Transition was fixed near the leading edge at $x/c = 7\%$ on both sides of the airfoil. The test chamber dimensions were $0.78 \times 0.78\,\mathrm{m}^2$.

In this study, computational conditions which are followed is shown in Table I.

Table I. Computational conditions.

M_∞	α	Re/m	T_i
0.73	4°	10.5×10^6	300 K

3. COMPUTATIONAL RESULTS

3.1. Validation of turbulent model

Before performing computation of transonic flow around OAT15A ONERA airfoil, it is important to evaluate the ability of the turbulence model to compute classical configurations. For this reason, computation of turbulent boundary layer at Mach number of 0.6 was performed. Figure 1 presents results of this model compared to the log law. It can be seen that the model gave approximately the same results and trends as the analytical law. This confirms the fact that the turbulent model is able to compute this steady turbulent case.

Figure 2 presents turbulent kinetic energy, turbulent viscosity and turbulent viscosity coefficient. It can be seen that turbulent kinetic energy is large near the wall ($y < 0.015$) and it is the maximum. The turbulent viscosity is also large near the wall and presents a maximum located at $y = 0.006$. An important result is the value of $C\mu$ in the equilibrium region which is equal to 0.085 for $0.0012 < y < 0.01$. This value is not very different from 0.09, the classical value usually used by the standard turbulent model. This result shows that the model is able to find automatically the right value in the equilibrium zone. So this confirms the fact that the present model can be used for equilibrium turbulence.

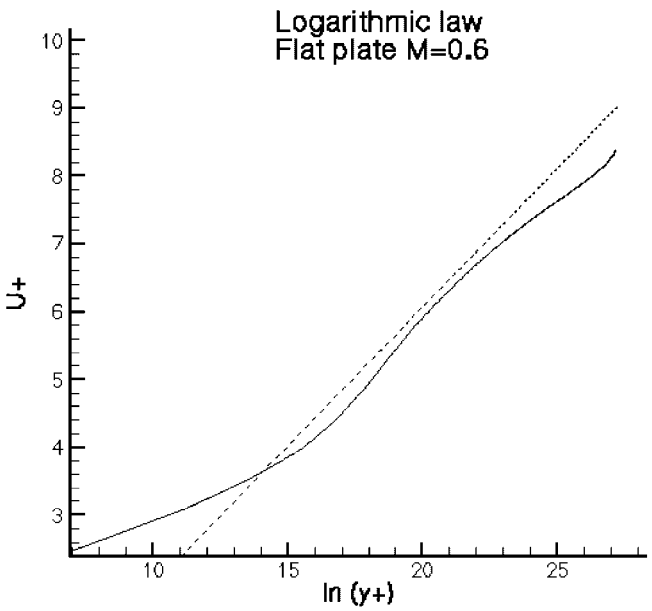

Figure 1. Turbulent boundary layer at $M = 0.6$.

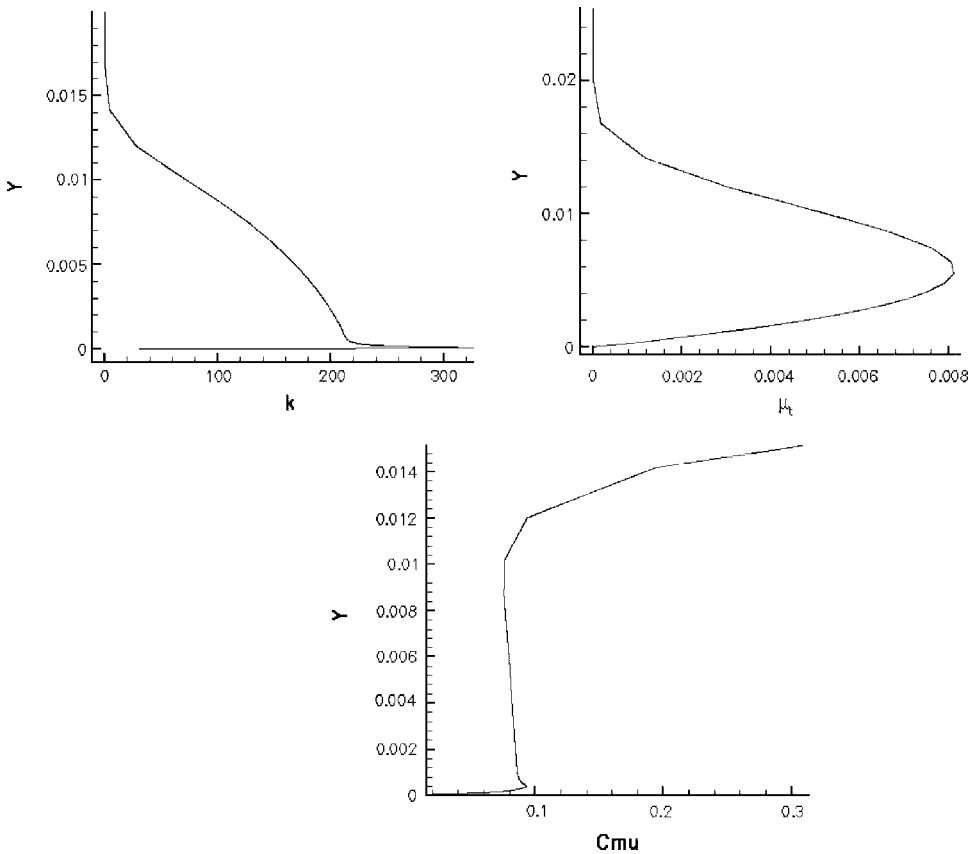

Figure 2. Turbulent boundary layer at $M = 0.6$; k, μ_t and $C\mu$.

The second test case computed is an unsteady one. It is the well known separated incompressible flow around a NACA0012 airfoil. The Reynolds number computed is equal to 240.000 and the transition point is fixed at $x/c = 2.5\%$. Figure 3 shows the lift coefficient obtained with the present model compared to the experimental results (provided from DSO Singapore). It can be seen that the agreement is very good. The separation and stall points are well predicted. In spite of the fact that the lift is over estimated for $\alpha = 15^\circ$ and 20°, it is well predicted for the other incidences.

To summarize, the present model can be used to compute subsonic flows, both steady and unsteady, now it will be tested to compute transonic flow over an airfoil that contains unsteady oscillations, shock displacement and shock wave/boundary layer interactions.

3.2. Transonic flow around airfoil: buffeting phenomena

For this numerical computation, to minimize numerical diffusion and to ensure an acceptable one, the time step selected is $\Delta t = 5 \times 10^{-6}$. Figure 4 presents the pressure coefficient around the airfoil. It can be seen that the displacement of the shock upstream and downstream is

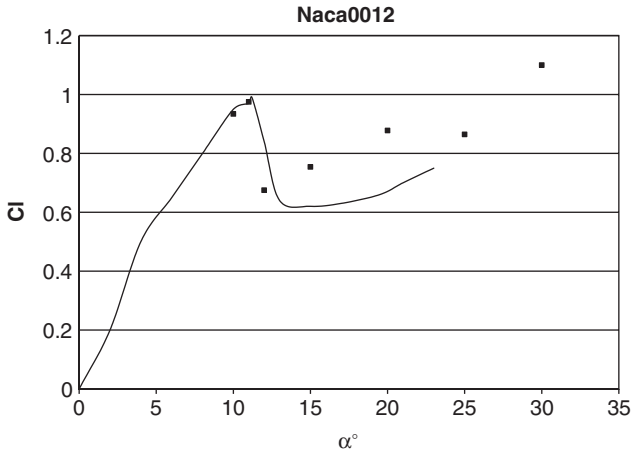

Figure 3. Lift coefficient (solid line: experiment, symbols: present computation).

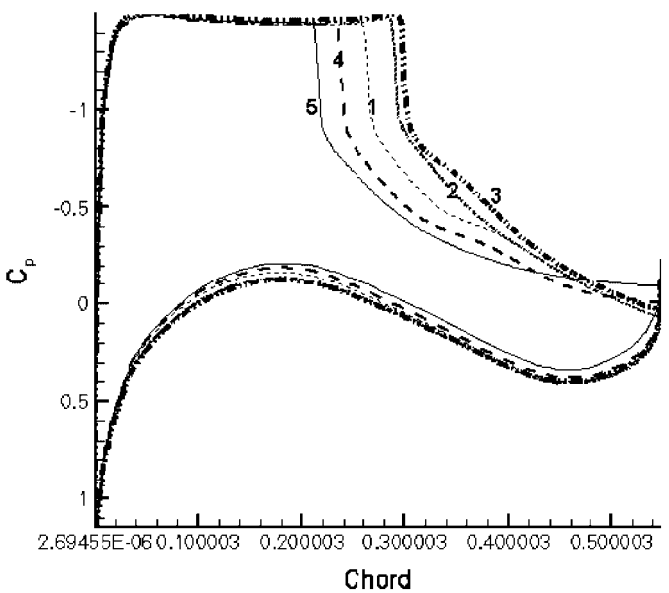

Figure 4. Pressure coefficient around airfoil (1: T0, 2: T0+T/6, 3: T0+T/3, 4: T0+2T/3, 5: T0+5T/6).

captured. Also, at the trailing edge, the separations related to the shock wave/boundary layer interaction can be observed. Both the motion of the shock wave location and size of the separation are correlated. Figure 5 shows the rms pressure. The present model presents good agreement with experimental results [4–6]. In the same figure numerical results obtained by ONERA with algebraic Reynolds stress model (ARSM) are presented [14, 15] (more complex model, with more equations and more computational time). This computation also presents

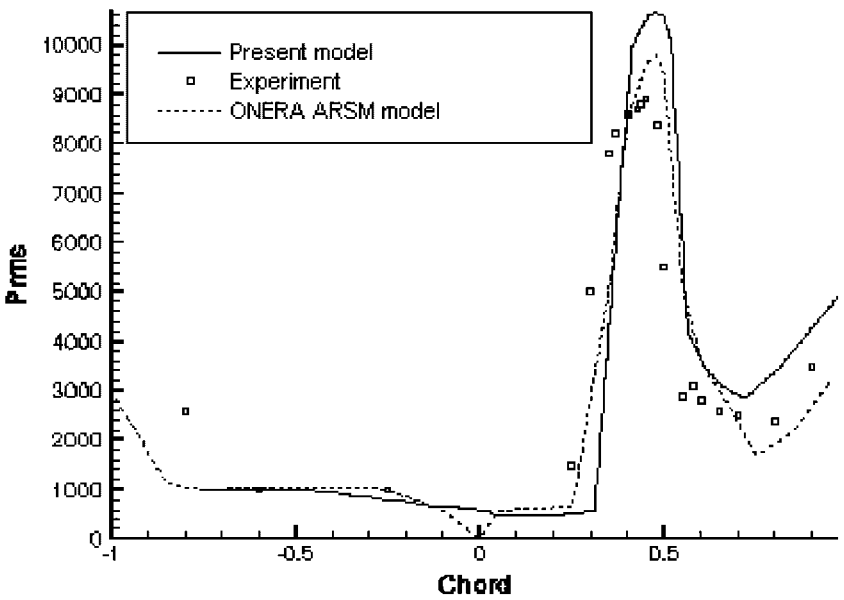

Figure 5. RMS pressure.

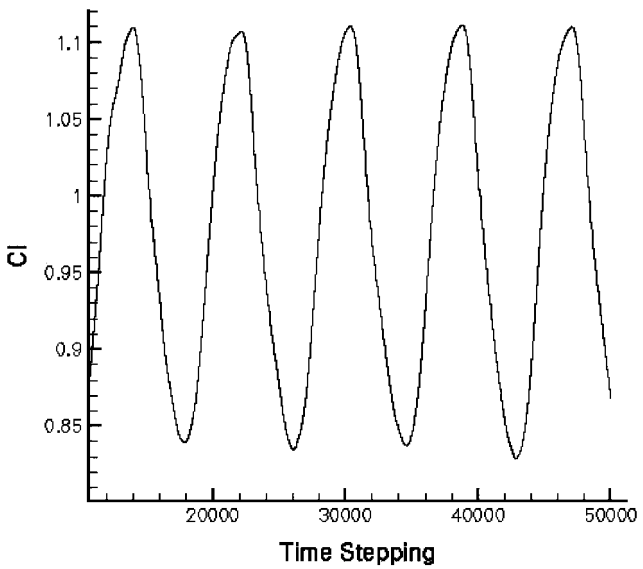

Figure 6. Time evolution of lift coefficient.

good agreement. However, it was not possible to correctly describe these phenomena with the standard model (constant $C\mu$). The time history of a lift coefficient is presented in Figure 6 for t as between 0 and 025 s. It can be seen that the evolution is unsteady and periodic. This evolution is in agreement with experimental measurements and observations. The Strouhal

Table II. Comparison with experiment and other computation.

Case	Non-dimensional frequency	Mean lift coefficient
Experimental results ($\alpha = 3.91°$) [4–6]	0.078	0.91
ONERA Computation ($\alpha = 4°$) [14, 15]	0.074	0.97
Present study ($\alpha = 4°$)	0.072	0.965

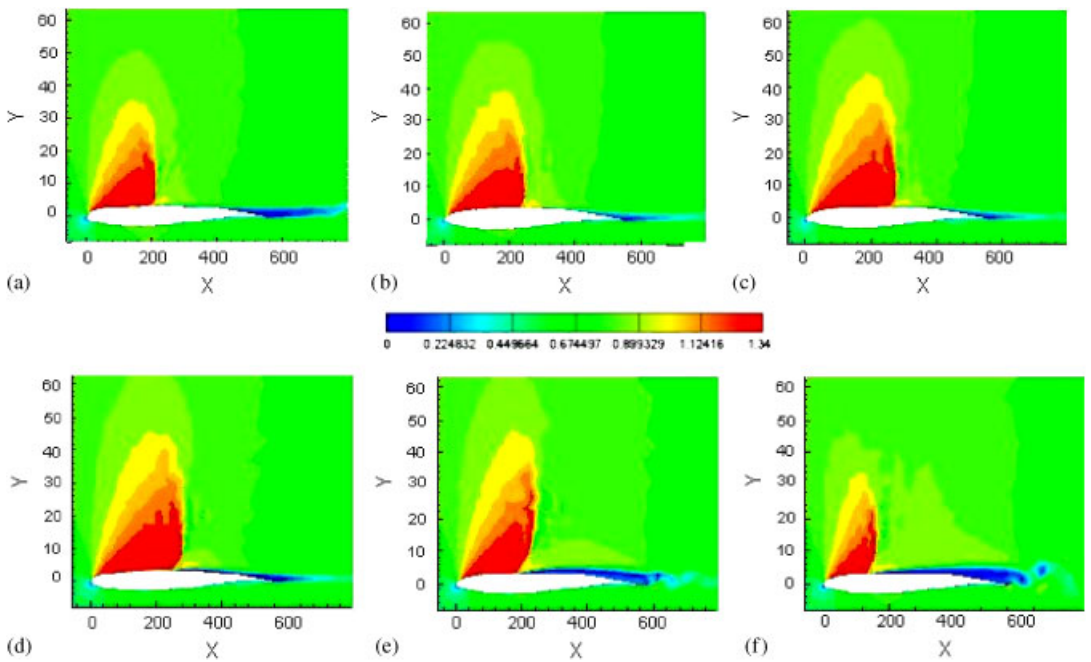

Figure 7. Iso-Mach number during one period (maximum Mach number = 1.34): (a) T0; (b) T0+T/6; (c) T0+T/3; (d) T0+T/2; (e) T0+2T/3; and (f) T0+5T/6.

number obtained, $St = fc/U_\infty = 0.072$, is approximately the same value obtained in the other studies as can be observed in Table II. Table II has also compared the mean lift coefficient. The coefficient obtained has approximately the same value as the other studies. The Strouhal number and the corresponding frequency is the one related to the displacement of the shock. In the wake another periodic phenomenon is detected and is the von-Karman instability. This mechanism is the same as the one analysed by Bourdet *et al.* [16] and Bouhadji and Braza [17–19] in the case of the NACA0012 wing with the help of a 3D DNS. In the present case the von-Karman street instability correspond to a Strouhal number of 2.75.

Flow visualization of iso-Mach number during one period of shock displacement is given in Figure 7. The displacement of shock waves can be observed. The shock wave/boundary

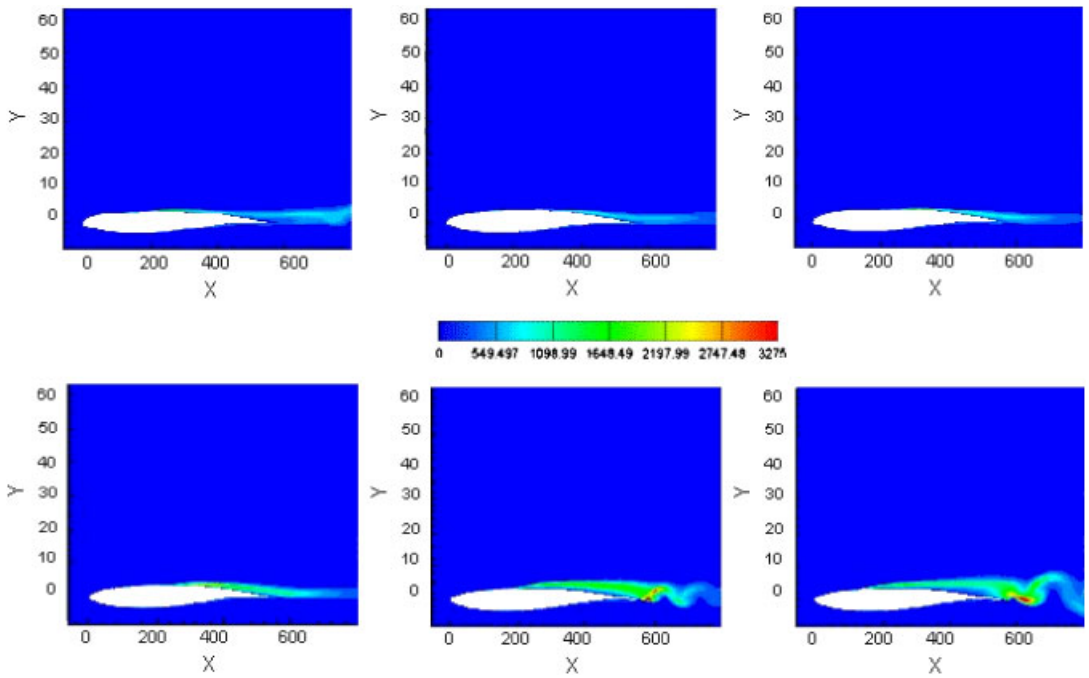

Figure 8. Iso-kinetic turbulent energy during one period (corresponding to Figure 7).

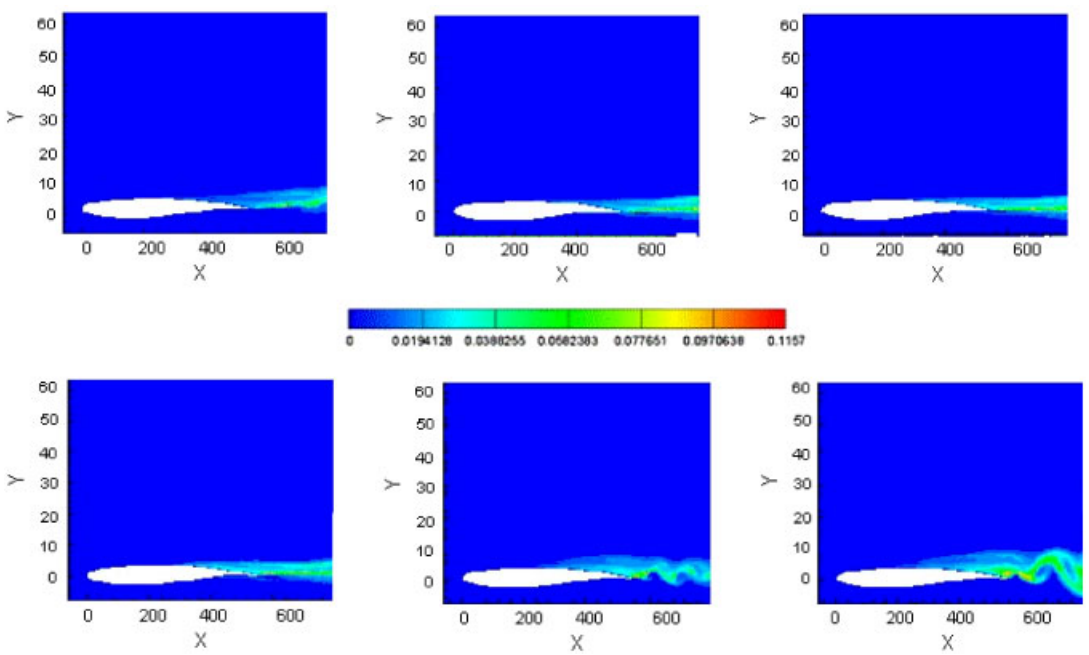

Figure 9. Iso-turbulent viscosity (μ_t) during one period (corresponding to Figure 7).

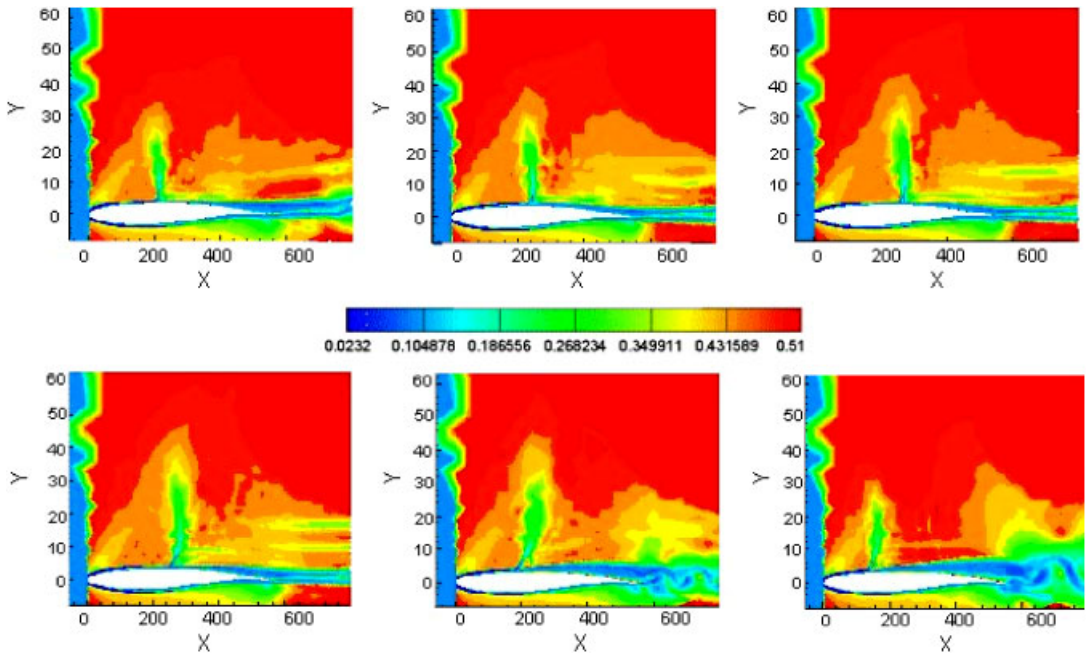

Figure 10. Iso-turbulent viscosity coefficient ($C\mu$) during one period (corresponding to Figure 7).

layer interaction characterized by the occurrence of separation can be noticed. During the first half of the period, the shock wave moves downstream (Figure 7a–c). For the second half it moves upstream (Figure 7d–f). The separation resulting from the shock wave/boundary layer interaction occurs in this figure at time station a, d, e and f and is important at time station e and f. When shock moves downstream, the separation zone decreases and disappears. A separation zone increase leads to an upstream shock displacement. Downstream of the separation, in the wake, the beginning of the von-Karman street can be noticed (e and f). All these unsteady phenomena can be observed in the movie obtained by flow visualization. The maximum Mach number is equal to 1.34.

Figures 8–10 present, respectively, the turbulent kinetic energy (k), the turbulent viscosity (μ_t) and the turbulent viscosity coefficient ($C\mu$). Both the turbulent kinetic energy and turbulent viscosity are important near the trailing edge and in the wake. The maximum turbulent kinetic energy, obtained from this figure, is equal to 3275 J and the maximum turbulent viscosity is $0.1157\,\mathrm{m}^2/\mathrm{s}$. The variation of $C\mu$ is important in the same region as the other turbulent variables but also in the shock wave region, as can be noticed in Figure 10. The variation of this coefficient is between 0.0232 and 0.51.

4. CONCLUSIONS

A numerical study was conducted to investigate the oscillations resulting from a transonic shock wave/boundary layer interaction. To perform this computation OAT15A ONERA airfoil

is selected. In these situations, the following conclusions can be made:

- Concerning turbulence modelling, from the present simulations, it can be concluded that the turbulence model developed is able to capture the global features of the flow and to provide necessary fidelity to quantify the unsteady flow developed when shock wave/boundary layer interaction and separation take place.
- The unsteady mechanism resulting from the shock wave/boundary layer interaction is analysed. First the shock wave position is unsteady and it moves downstream. Separation also moves with this displacement. When the flow is separated, in the wake another unsteady mechanism, the von-Karman instability is observed. Frequencies and levels of this phenomenon are well predicted.

ACKNOWLEDGEMENTS

This work is part of the research program managed by GDR2502 "Contrôle Des Décollements" (Separation Control) of CNRS.

REFERENCES

1. Lee BHK. Oscillatory shock motion caused by transonic shock boundary-layer interaction. *AIAA Journal* 1990; **28**(5):942–944.
2. Lee BHK, Murty H, Jiang H. Role of Kutta waves on oscillatory shock motion on an airfoil. *AIAA Journal* 1994; **32**(4):789–795.
3. Girodroux-Lavigne P, Le Balleur JC. Unsteady viscous-inviscid interaction method and computation of buffeting over airfoils. *Joint IMA/SMAI Conference on Computational Method in Aeronautical Fluid Dynamics*, University of Reading, MA, 6–8 April 1987.
4. Naudin P, Guimarey E. Measures instationnaires sur un profil OAT15A à S3Ch. *PV 6/05626 DAAP/DAFE*, novembre 2002.
5. Molton P, Jacquin L. Etude de l'écoulement instationnaire autour d'un profil transsonique OAT15A. Soufflerie S3Ch. *PV 187/05626 DAAP/DAFE*, avril 2003.
6. Maury B. Etude de l'écoulement instationnaire autour d'un profil transsonique OAT15A. Soufflerie S3Ch. *PV 186/05626 DAAP/DAFE*, juillet 2003.
7. Kourta A. Instability of channel flow with fluid injection and parietal vortex shedding. *Computers and Fluids* 2004; **33**(2):155–178.
8. Chalot F, Mallet M, Ravachol M. A comprehensive finite element Navier–Stokes solver for low and high-speed aircraft design. *AIAA 94-0814*.
9. Petit G, Rosenblum JP, Courty JC, Kourta A. Ecoulements turbulents instationnaires décollés et contrôle sur un profil. *39ème Colloque d'Aérodynamique Appliquée*, *Contrôle des écoulements*, Paris, 22–24 mars 2004.
10. Zhu J, Shih T. Computation of confined coflow jet with three turbulence models. *International Journal of Numerical Methods in Fluids* 1994; **19**:939–956.
11. Shih T, Zhu J, Lumley J. A realizable Reynolds stress algebraic equation model. *NASA TM 105993*, 1993.
12. Lumley J. Computational modeling of turbulent flows. *Advances in Applied Mechanics* 1978; **18**:124–176.
13. Kourta A. Computation of vortex-shedding in solid rocket motors using time-dependent turbulent model. *Journal of Propulsion and Power* 1999; **15**(3):390–400.
14. Brunet V. Simulation numérique par l'approche URANS des instabilités aérodynamiques en régime transsonique. *Rapport technique de synthèse ONERA DAAP*, novembre 2003.
15. Brunet V. Computational study of buffet phenomenon with unsteady RANS equations. *AIAA 2003-3679*, Orlando, FL.
16. Bourdet S, Bouhadji A, Braza M, Thiele F. Direct numerical simulation of the three-dimensional transition to turbulence in the transonic flow around a wing. *Flow Turbulence and Combustion* 2003; **71**:203–220.
17. Bouhadji A, Braza M. Compressibility effect on the 2D and 3D vortex structures in transonic flow around a wing. *ERCOFTAC Bull*. 1997; **34**:4–9.
18. Bouhadji A, Braza M. Organised modes and shock-vortex interaction in unsteady viscous transonic flows around an aerofoil. Part I: Mach number effect. *Computers and Fluids* 2003; **32**(9):1233–1260.
19. Bouhadji A, Braza M. Organised modes and shock-vortex interaction in unsteady viscous transonic flows around an aerofoil. Part II: Reynolds number effect. *Computers and Fluids* 2003; **32**(9):1261–1281.

